STUDIES OF DAMPING RING LOW EMITTANCE TUNING

J. Jones
STFC, Daresbury Laboratory, UK

Abstract

The deliverables of the Low Emittance Tuning task, as part of the Damping Ring work package, are presented.

As part of the ongoing ILC damping ring design study, simulations have been performed on the methods of tuning the low vertical emittance to the required levels under the presence of errors. The effects of both static alignment errors, as well as long term ground drift are investigated.
The simulations show that the current damping ring design performs well under the investigated error sources and that the damping ring should meet its specifications in terms of extracted vertical emittance in most cases.

1 Introduction

The ILC luminosity is strongly dependant on the vertical emittance achievable at the IP. This must be orders of magnitude less than can be produced at the electron or positron sources. The ILC damping rings are therefore designed to provide this orders of magnitude reduction in the vertical emittance through radiation damping processes. The natural radiation damping in the ring is augmented by many hundreds of meters of damping wiggler. The large size and complex nature of both the damping ring lattice and the damping wigglers means that the achievable emittance is very sensitive to errors in the system.
These errors can be broadly split into static errors and dynamic errors. Both include deviations of the magnets away from their nominal position, as well as variation in the magnetic field strengths of the main field and other error fields.
The specification for the damping ring extracted emittance has been set at 20nm-rad, normalised at an energy of 5GeV. This will be the benchmark figure throughout this report.
This report will investigate these effects for the latest design damping ring lattice.

2 Method

This report investigates the latest ILC Damping Ring lattice, so-called DCO2 [i]. This lattice contains all required elements used for correction of the damping ring.
The damping ring lattice has been input into the Mathematica based MADInput programming language. Analysis of the lattice dynamics is then performed through the MAD8.23dl optics code.

The final lattice used through-out this note contains 690 beam position monitors, as well as 690 closed-orbit correction dipole magnets. The lattice notionally contains 376 skew quadrupoles.

In all cases described, the extracted vertical emittance is given as an r.m.s value, calculated over 50 random seeds.

2.1 Errors

Analysis of static errors is performed simply using commands internal to the mad code. Analysis of dynamic effects such as ground motion, both ATL like and elastic-wave like, are interfaced though the MADInput engine.
The underlying principles surrounding the simulation of dynamic ground motion effects are described in [ii][iii].
Although definitions for girders in the damping ring have not been specified, a small number of defined girder elements have been assumed for this study. Correctors, BPMs and their associated quadrupole or sextupole are assumed to be on the same girder. Damping wigglers are likewise assumed to be on girders, reflecting the likely physical construction of these devices.
The final ATL covariance matrix is 2926x2926 elements. Motion is added randomly at each different time step. A representative example of ATL ground motion applied over 50 hours is shown in Figure 1.

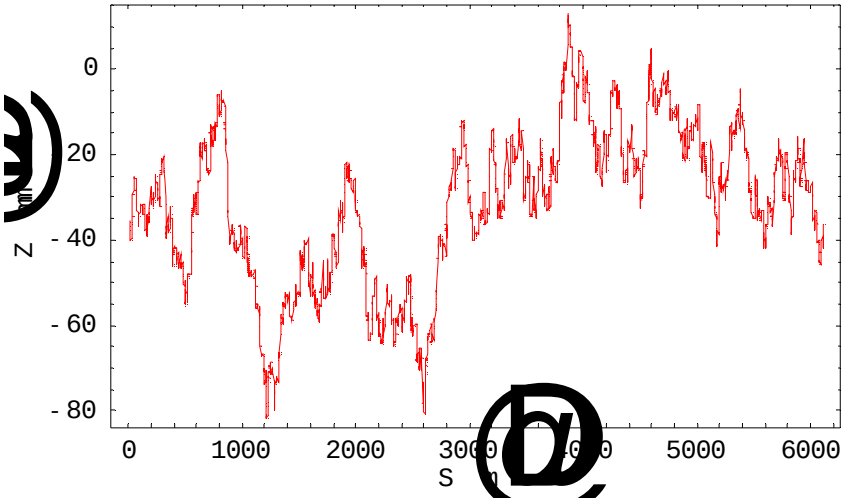

Figure 1 Example of ATL motion as applied to the damping ring, over a time frame of 50 hours and with an A-value of 10^{-17} meter second^{-1}.

2.2 Closed-orbit correction

Closed orbit correction is performed using a Singular Value Decomposition based method [iv]. Analysis and construction of the inverse response matrices is performed in Mathematica. The singular values, $\sigma_{x,y}$, in both planes are plotted in Figure 2.

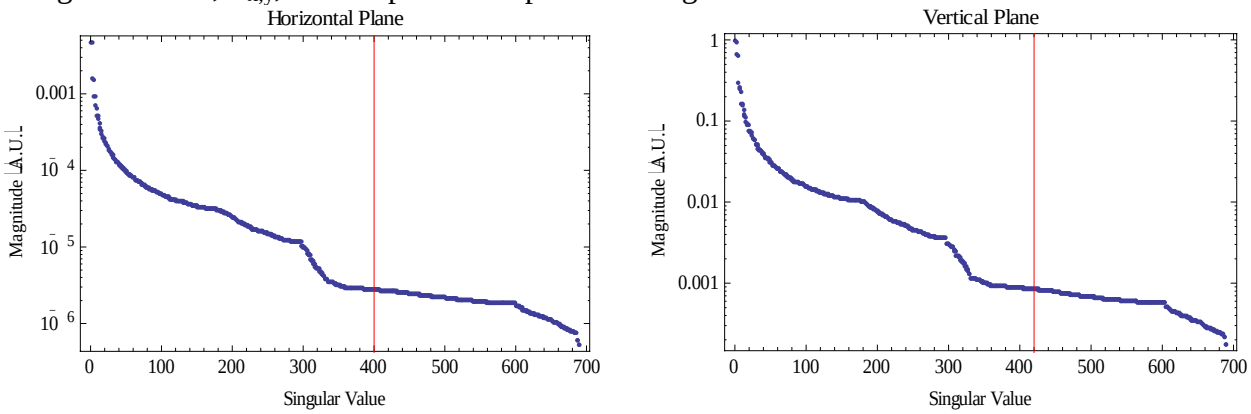

Figure 2 Closed orbit response matrix singular values in both horizontal (left) and vertical (right) planes, highlighting the relevant singularity rejection parameter (red vertical line).

All corrector magnets and BPMs are included in the analysis. In the horizontal plane, 400 eigenvalues were retained in the matrix inversion, while in the vertical plane 420 were retained.

2.3 Vertical dispersion and coupling correction

Vertical dispersion correction can be performed using either the dipolar correctors used in the closed-orbit correction, or the skew quadrupoles used for coupling correction. Previous studies [v] have shown that the vertical emittance is reduced using skew quadrupoles for the vertical dispersion correction.

For this analysis vertical dispersion and coupling correction were combined. In an analogous fashion to the closed orbit correction, the combined correction is performed via a simple SVD based inversion of a vertical dispersion+coupling response matrix. The correctors in this case are skew quadrupoles placed near to the sextupoles in the lattice.

The dispersion part of the response matrix is simply the measured vertical dispersion at each BPM. The vertical dispersion is determined from the change in vertical orbit at two different energies. This was arbitrarily chosen to be ±1% of the reference beam energy. In the real damping ring this will

need to be a careful balance between required BPM accuracy, and non-linear effects introduced with off-momentum beams.
The coupling response is the change in vertical orbit as 4 independent *horizontal* kicks are applied in the machine. The magnitude of the *vertical* orbit provides some correlation to the linear coupling in the machine.
The 4 horizontal kickers were chosen from the set of corrector magnets in the lattice. The kickers were chosen based on their relationship between the phases in the two transverse modes. A pair of kickers with a difference phase of $\nu_1 - \nu_2 = \frac{n\pi}{2}$, n odd, and a separate pair with a sum phase of $\nu_1 + \nu_2 = \frac{n\pi}{2}$, n odd, were chosen.
All BPMs were used in the measurement of the vertical coupled orbit and the dispersion.
Due to the different magnitudes of motion for the dispersive and coupling response-matrix elements, the two components need to be normalised. Investigations showed that a value of 0.11*η_y produced a reasonable compromise between vertical-dispersion correction and coupling correction.
The singular values for the vertical dispersion+coupling response matrix are given in Figure 3.

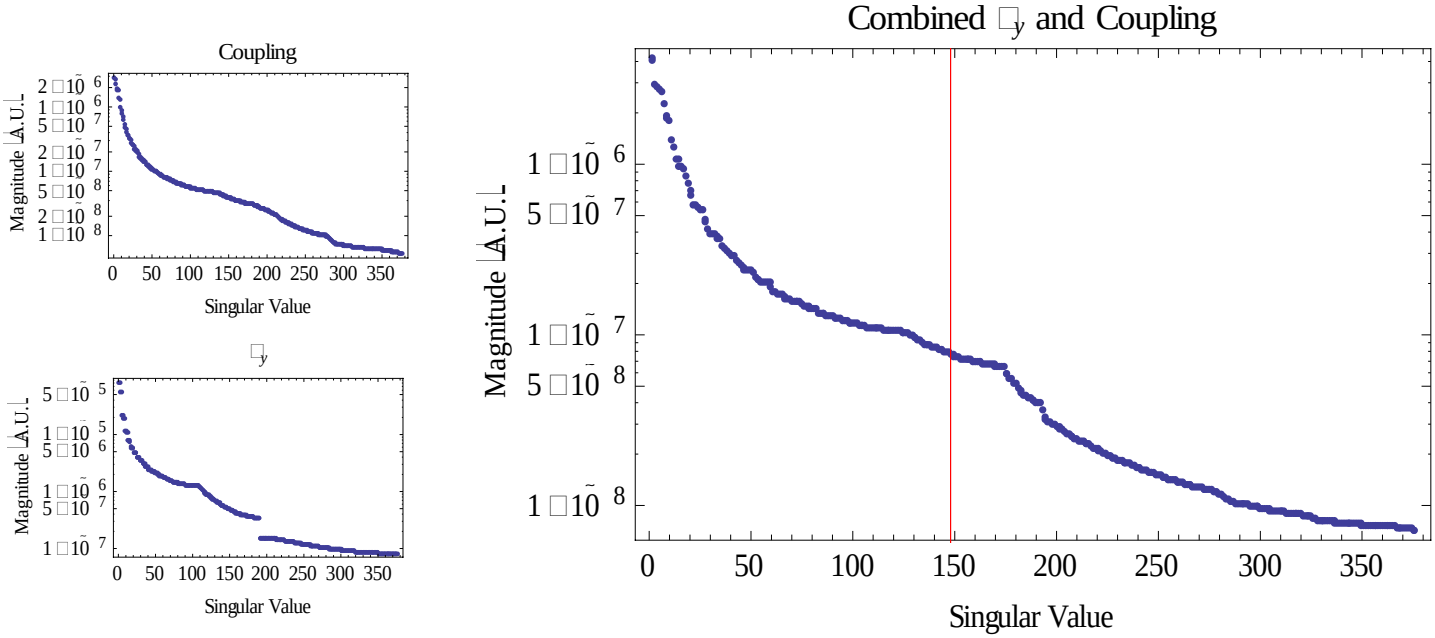

Figure 3 Coupling (left, top) and vertical dispersion (left, bottom) singular values. The combined matrix singular values (right) is shown with a normalisation factor of 0.11 η_y. The singularity rejection parameter is also highlighted (red vertical line).

The singularity rejection criterion was taken to be 148 Eigenvalues for the combined matrix.

3 Results

3.1 Static Position errors

The tolerances for the damping ring are analysed in terms of a set of standard errors. These errors are based on expected alignment tolerances of the magnetic elements of the damping ring. They are given in Table 1.

Table 1: Standard Alignment Errors

	Δx (μm)	Δy (μm)	ΔRotation (around S axis) (mrad)
Quadrupole	30	30	0.3
Sextupole	30	30	0.3

BPM	100	100	20

The errors are applied as 3σ truncated Gaussian distributions to all relevant elements in the machine.

3.1.1 All Errors Tolerances

The tolerance of the DR to the alignment tolerances given in Table 2 are shown in Figure 4.

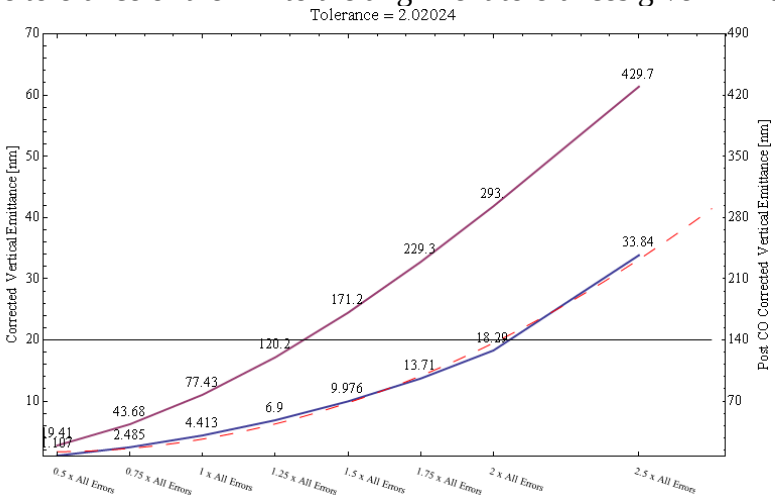

Figure 4 The r.m.s standard errors leading to an r.m.s emittance of 20nm-rad. The red line indicates the vertical emittance after C.O. correction, while the blue line indicates the vertical emittance after full correction, the red-dashed line provides a simple 2nd-order fit to this.

The figure clearly illustrates that the standard errors produce an extracted vertical emittance that is well below the tolerance of 20nm. The standard machine with full correction can accept a factor of 2 increase in errors, in the r.m.s sense.

3.1.2 Quadrupole Roll Tolerance

The tolerance for the quadrupole roll angle around the s-axis is given in Figure 5. The roll of the quadrupoles directly leads to coupling in the beam as well as an increase in the vertical dispersion.

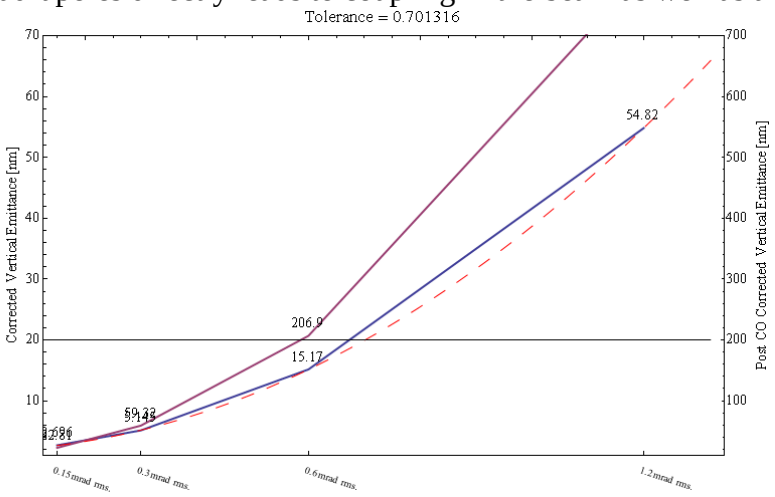

Figure 5 The r.m.s vertical quadrupole rotation leading to an r.m.s emittance of 20nm-rad. The red line indicates the vertical emittance after C.O. correction, while the blue line indicates the vertical emittance after full correction, the red-dashed line provides a simple 2nd-order fit to this.

3.1.3 Sextupole Vertical Alignment

The sextupole tolerance for vertical transverse motion is shown in Figure 6. Vertical motion of the sextupoles directly leads to an increase in the coupling of the beam.

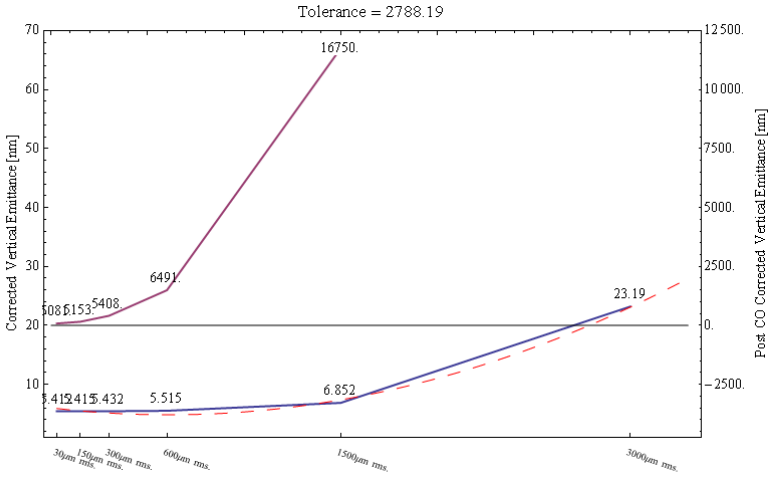

Figure 6 The r.m.s sextupole vertical motion leading to an r.m.s emittance of 20nm-rad. The red line indicates the vertical emittance after C.O. correction, while the blue line indicates the vertical emittance after full correction, the red-dashed line provides a simple 2nd-order fit to this.

The figure clearly shows the tight tolerances on the sextupole vertical motion without coupling correction.

3.1.4 BPM Vertical Alignment

The Beam Position Monitor tolerance for vertical transverse motion is shown in Figure 7. Alignment of the beam position monitors to the nominal axis of the machine provides the lower limit on the vertical beam offset in the quadrupoles and the sextupoles, which leads to an increase in both the vertical dispersion and the coupling in the machine.

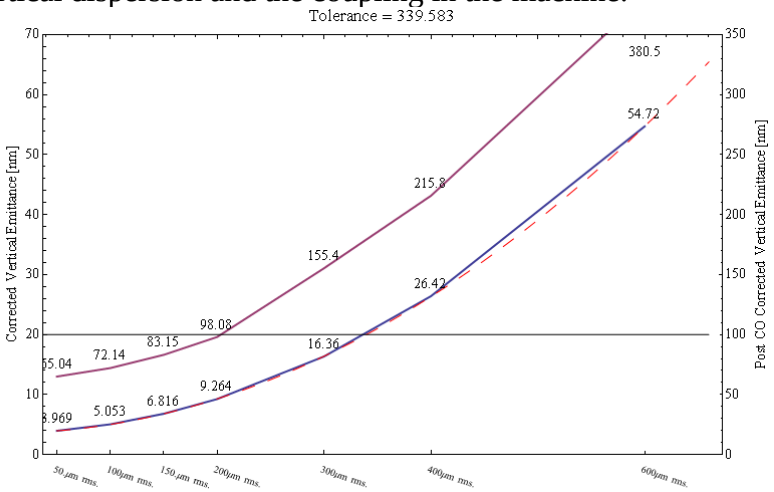

Figure 7 The r.m.s beam position monitor vertical alignment leading to an r.m.s emittance of 20nm-rad. The red line indicates the vertical emittance after C.O. correction, while the blue line indicates the vertical emittance after full correction, the red-dashed line provides a simple 2nd-order fit to this.

3.1.5 BPM Rotational Alignment

The Beam Position Monitor tolerance for rotation around the S-axis is shown in Figure 8. Rotation of the BPMs produces a spurious coupling signal, as well as somewhat limiting the closed-orbit correction.

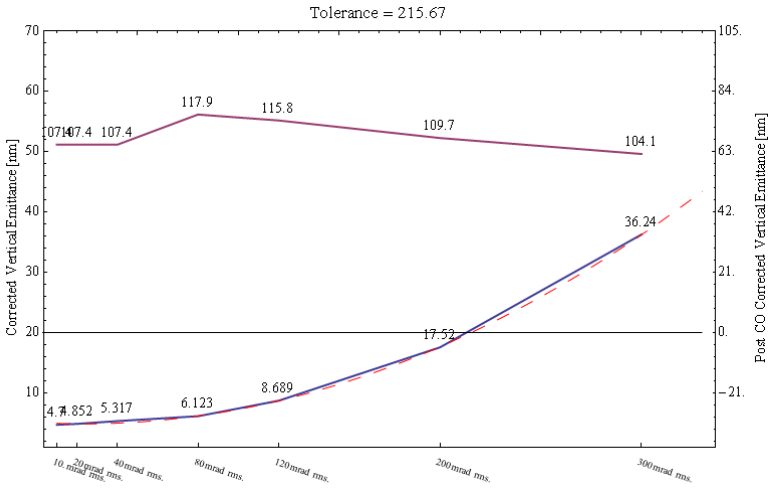

Figure 8 The r.m.s beam position monitor rotational alignment leading to an r.m.s emittance of 20nm-rad. The red line indicates the vertical emittance after C.O. correction, while the blue line indicates the vertical emittance after full correction, the red-dashed line provides a simple 2nd-order fit to this.

4 ATL ground motion

To investigate the effects of ATL style ground motion on the DR emittance tuning procedure, the machine was investigated over a period of time, under the influence of time evolved ground motion. Two cases were investigated:

1. With orbit and vertical dispersion and coupling correction performed once per day
2. With full low emittance tuning performed at the start, and the machine allowed to move with no more correction.

At the start of the studies, standard alignment tolerances are applied to the machine. During any correction procedures the machine is allowed to move under the influence of ground motion between the measurement and correction, which is assumed to take 1 minute in all cases.

The amplitude of the ground motion is 100μm/10m/year, a figure representative of that seen at 3rd generation synchrotron light sources around the world [vi]

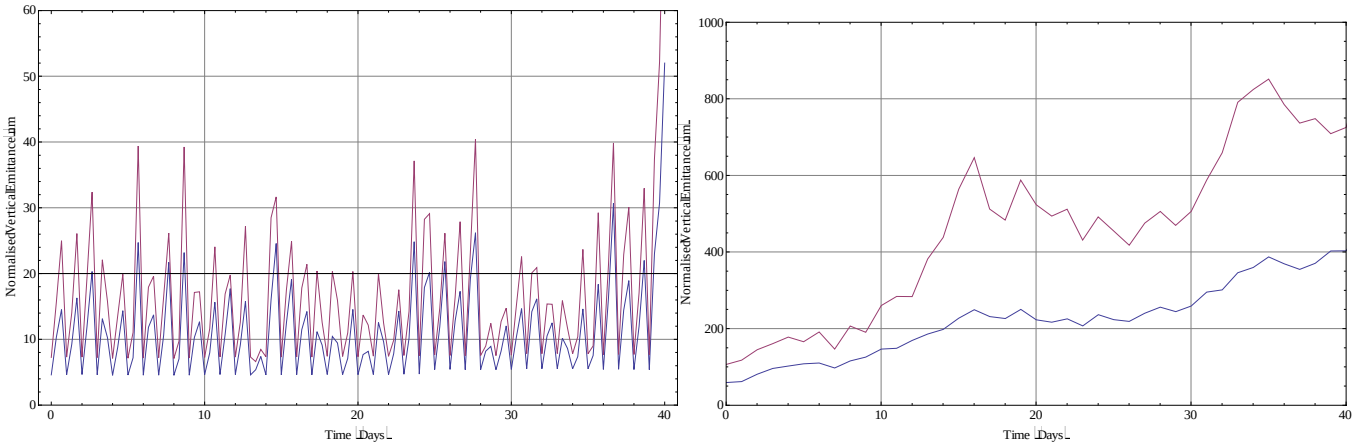

Figure 9 Plot of the normalised emittance from the damping ring over time under the influence of ATL ground motion. The r.m.s (blue) and the 95% Gaussian confidence limit (magenta line) are shown, for 15 random seeds. **Left:** Full closed-orbit and vertical dispersion and coupling correction is performed once per day. **Right:** No Correction.

Figure 9 clearly shows that the r.m.s vertical emittance is kept close to the required emittance with correction only once per day. Correction at intervals less than this should be enough to maintain the vertical emittance to less than 20nm. The interval required for correction places limits on the time taken to perform the correction, and so minimise the disruption on the rest of the machine.

5 Investigating the Number of Required BPMs

It is instructive to investigate the number of beam position monitors required to perform adequate low emittance tuning in the damping rings. The beam position monitors provide all of the information used in the tuning algorithms described above, and therefore are of vital importance to the ability of the tuning algorithms to meet the requirement of 20nm extracted emittance.
There are several strategies to reduce the number of BPMs in the lattice.

5.1 Methods

5.1.1 General

In all of the following cases, the extracted emittance is calculated as an r.m.s over 20 random seeds. When the number of BPMs in the lattice is reduced, the correction response matrices need to be re-calculated with the reduced number of BPMs. In this case all of the matrices required were re-inverted. As there are fewer BPMs, the required number of eigenvalues retained in the inversion changes. For this study, the number of rejected eigenvalues is determined by removing those eigenvalues with values fractionally less than the largest eigenvalue. For the closed-orbit correction matrices, the fraction is 0.001, and for the vertical dispersion and coupling matrix, it is 0.0029. These factors give the correct number of eigenvalues in the inversion if all BPMs are present.

5.1.2 Systematically Removing BPMs

BPMs are removed from the lattice systematically, by removing, say, every other BPM. This strategy produces a uniform BPM distribution throughout the lattice. As the number of BPMs is reduced, the selection of BPMs in this systematic method can lead to a sensitivity to the choice of starting BPM, such that by changing this starting position the correction algorithm can perform markedly better or worse over a given set of errors in the machine. This is illustrated in Figure 10.

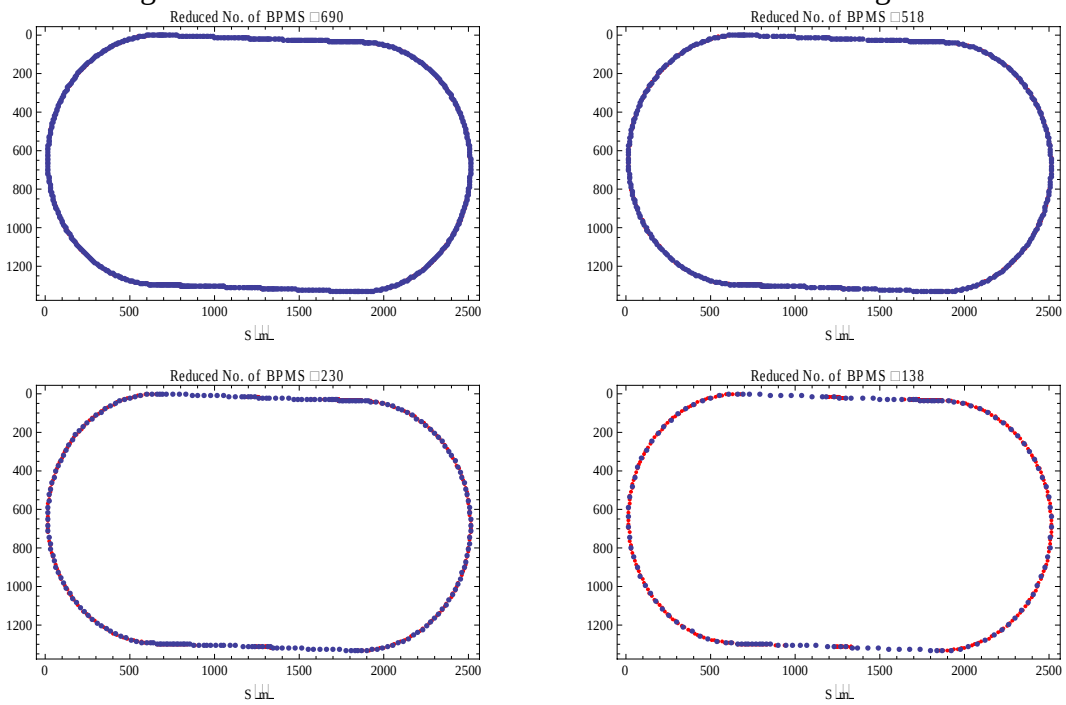

Figure 10 Plots of the position of BPMs (blue points) and synchrotron radiation sources (red points) for a different number of beam position monitors, based on a systematic reduction..

5.1.3 Removing BPMs at locations other than the radiation sources

The wigglers and bending dipoles in the damping ring lattice provide nearly all of the synchrotron radiation emission that drives the emittance damping and excitation processes. The vertical emittance

is increased by radiation emission at locations of high vertical dispersion. By maintaining beam position monitors at these radiation emission locations, and removing them elsewhere preferentially, it should be possible to maintain a low vertical emittance whilst reducing the total number of BPMs.

To investigate this method, BPMs were removed from the lattice systematically based both on their locations relative to dipole magnets in the lattice, and based on the density of nearby BPMs, thus maintaining good BPM coverage around the lattice, and preferentially removing BPMs further away from radiation sources. This is demonstrated in Figure 11. The locations of the wiggler magnets, which have a high density of radiation sources, can be seen in the lower right plot, where the remaining BPMs are clustered around these high density radiation locations.

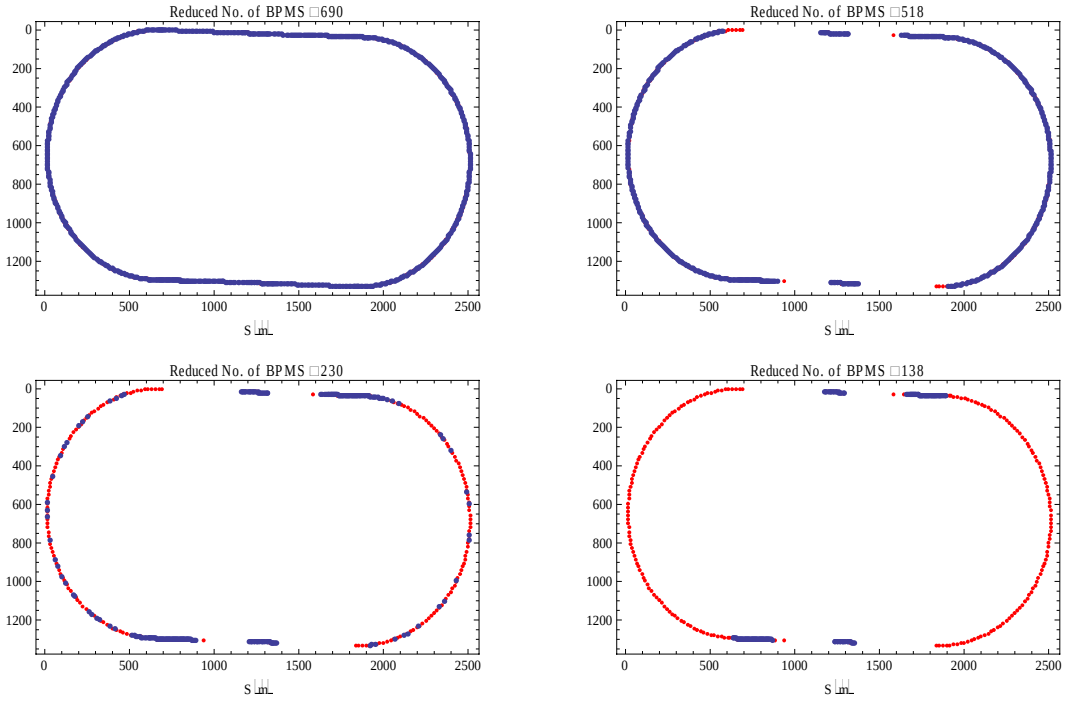

Figure 11 Plots of the position of BPMs (blue points) and synchrotron radiation sources (red points) for a different number of beam position monitors, based on proximity to the radiation sources. The wiggler magnets are clearly highlighted with the clustering of BPMs in the bottom right plot.

5.1.4 Analysis of the correction matrix eigenvalues

Inversion of the vertical dispersion and coupling response matrix using Singular Value Decomposition produces a matrix of the eigenvalues of the skew-quadrupole to BPM response system. These eigenvalues can be used to provide “efficiency” values for each of the BPMs in the system. The total number of BPMs can therefore be systematically reduced by removing BPMs with low “efficiency” values. Figure 12 show the position of the remaining BPMs as the least efficient are removed, for a different number of remaining BPMs. Comparison with Figure 11 shows that the most efficient BPMs are concentrated around the wiggler magnets, for similar reasons, but that there are more BPMs remaining in the long straight sections.

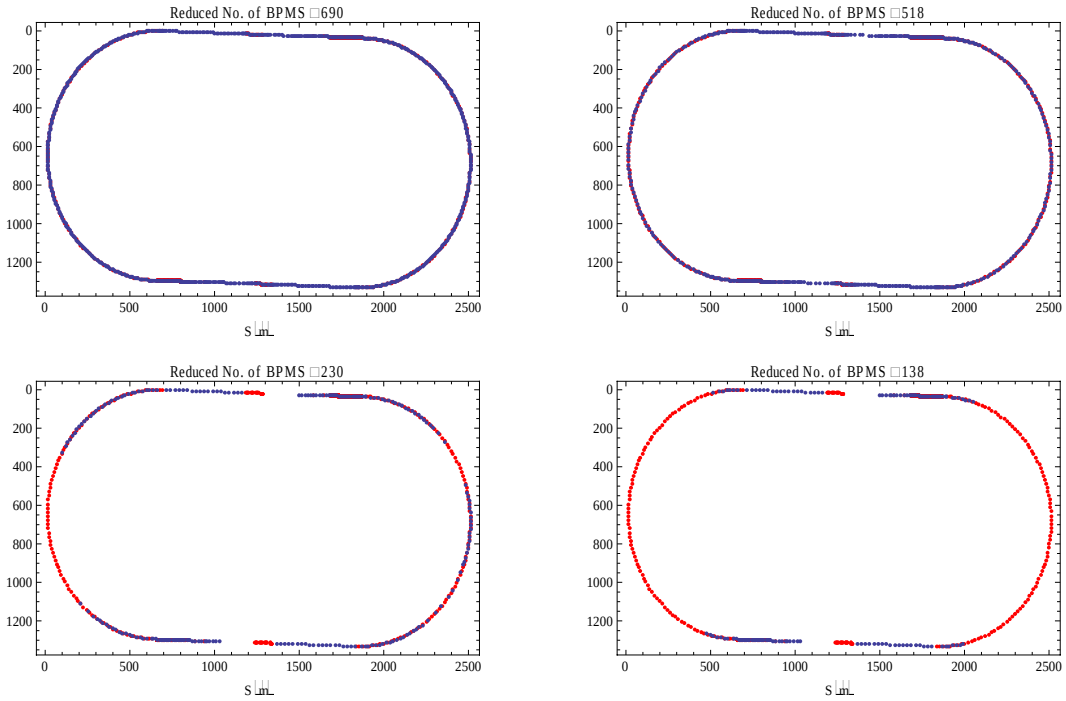

Figure 12 Plots of the position of BPMs (blue points) and synchrotron radiation sources (red points) for a different number of beam position monitors, selected based on the eigenvalues of the correction matrix.

5.2 Results

The results of the analysis are shown in Figure 13. It is clear from this plot that the best general solution to reducing the number of BPMs is a systematic reduction. However, better results can be obtained for a larger number of BPMs by initially removing only those with low “efficiencies”, as determined by the eigenvalues analysis. Reducing the number of BPMs based on their proximity to radiation sources does not seem to produce reasonable results. This is almost certainly due to the fact that the BPMs removed are not necessarily those that are best for emittance reduction. The relationship between the correction of the vertical emittance and the BPM position is inherently more complicated than is assumed in this case. Analysis of the BPM layouts in the eigenvalues and radiation source methods shows a similar distribution, but in the former case BPMs are removed based on their direct efficiency, rather than just on their proximity to the radiation sources.
As the number of BPMs in the lattice is reduced, it appears that a systematic, and therefore more uniform, distribution of BPMs produces lower final emittances. This highlights the wide variety of emittance degrading effects in the damping ring, that are not completely described by analysis of the greatest sources of synchrotron radiation – namely the wiggler magnets.
It is also clear from the plot that at low number of BPMs it becomes increasingly important exactly which BPMs are chosen. By rotating the position of the starting BPM, for the systematic case, wildly different r.m.s emittances can be observed.

The results tend to suggest that the minimum number of required BPMs is around 230 BPMs. This increases the extracted emittance by a factor of 2, but still leaves a factor of two emittance growth for other effects not explored in this report. For flexibility in the future it may be desirable to increase this number to around 345 BPMs, half of the originally specified number. This provides a reasonable compromise between extracted emittance and the additional costs incurred with a higher number of BPMs.

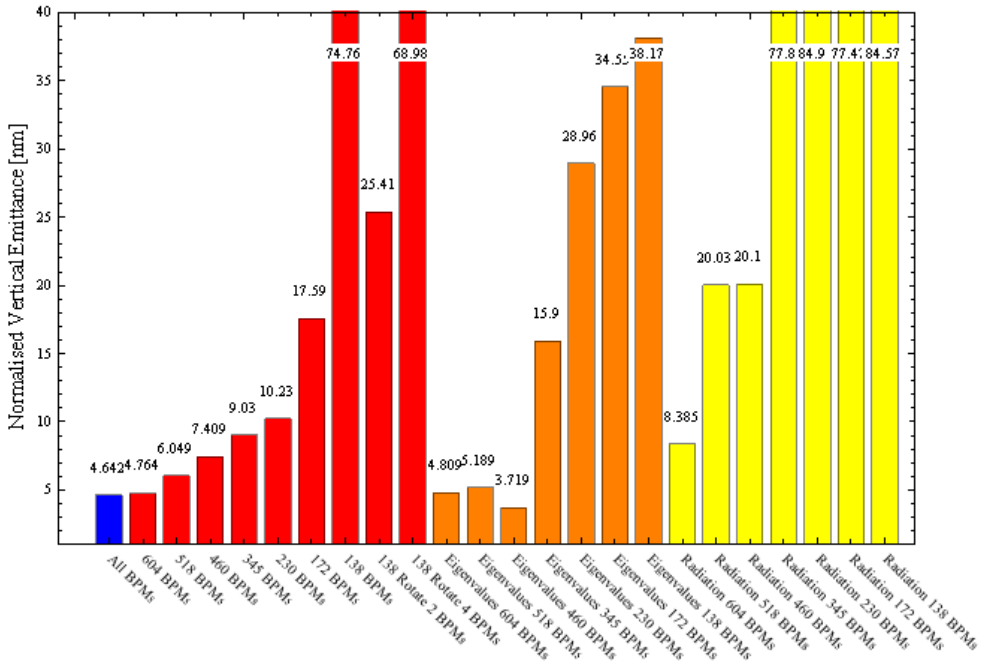

Figure 13 Extracted vertical emittance from the damping ring as a function of the number of BPMs in the lattice, and for the 3 different methods described above. The r.m.s vertical in each case is shown above the relevant bar.

6 Investigating the minimum number of required skew correctors

The number of skew-quadrupole correctors in the lattice also has a strong bearing on the efficiency of the correction algorithm, and its ability to reduce the extracted vertical emittance to the required 20nm value. In this case we investigate the extreme lower limits on the number of skew-quadrupoles for the lattice.

6.1 Method

The numbers of skew quadrupoles in the lattice are reduced by a systematic reduction by, say, removing every other magnet. This produces a lattice with a relatively uniform distribution of skew quadrupoles. As the investigation is looking at the limits on the number skew-quadrupoles, the tuning method is modified to produce the lowest vertical emittance possible, with no allowance for tuning time or other considerations. To perform this emittance tuning, a Nelder-Mead simplex algorithm is employed. This is a generalised non-linear optimisation algorithm, which contains no information on the lattice. The algorithm has as variables the skew-quadrupole strengths, and as a constraint the reduction of the calculated vertical emittance from the damping ring, as calculated by the normal lattice code. The algorithm varies the skew-quadrupole strengths until it achieves a vertical emittance of less then 20nm, at which point it stops. With more tuning time, it should therefore be possible to reduce the vertical emittance to lower values than presented here. Tuning time using this method takes order-of-magnitude longer than the correction algorithm described above, and so is not readily amenable to a real-life implementation. It is used here solely to understand the limits of the lattice emittance correction, with low numbers of skew-quadrupoles.

6.2 Results

The results of the simplex optimisation are shown in Figure 14. The results show that with standard errors, given in Table 1, it is possible to achieve the required vertical emittance of 20nm with only 2 skew quadrupoles. This is only true in an r.m.s sense however. With 6 skew-quadrupoles, all random seeds investigated achieved final emittances less than 20nm. The second plot shows that a 20nm

r.m.s vertical emittance is achievable with 5 skew-quadrupoles, with error amplitudes up to 3 times greater than the standard errors used throughout this note.
As noted above, however, the tuning times to achieve this are extremely long. In a realistic situation, one could reasonably expect the machine to have changed over the length of the tuning time, due to ground motion and other effects. These effects would probably limit the achievable emittances to greater than that demonstrated here.

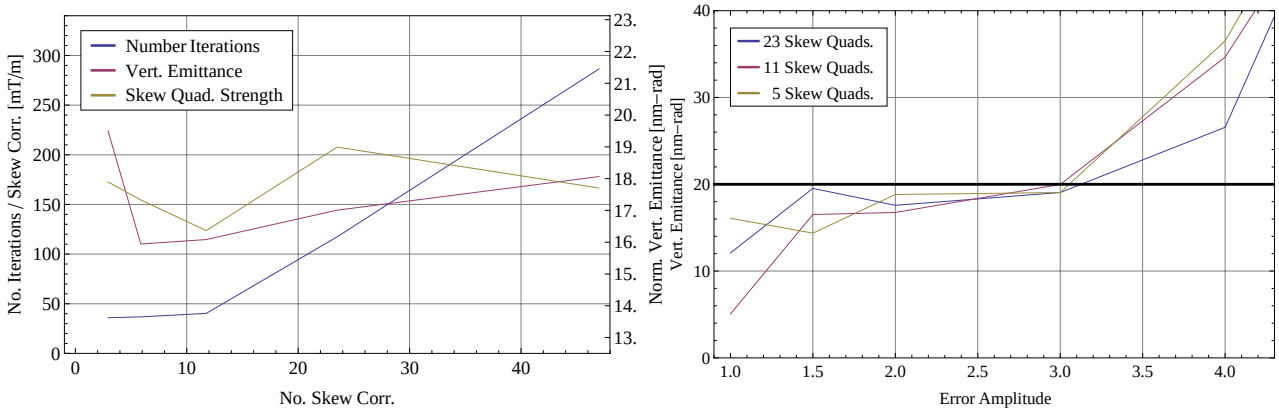

Figure 14 Plots showing the vertical emittance after simplex optimisation for varying numbers of skew quadrupoles with standard errors applied to the lattice (left) and the tolerance of the correction to varying amplitudes of errors, with different numbers of skew quadrupoles (right).

7 Investigating the use of dual-plane coupling response matrices

The algorithm for coupling given above uses the vertical response to a horizontal kick as a measure of the coupling. It is possible to generalise this method to look at the horizontal response from a vertical kick. Although it is primarily the vertical emittance that is important in the damping rings, the horizontal motion to a vertical kick also gives information on the coupling in the beam. By using the same 4 kickers as previously, but also kicking in the vertical plane, the amount of information is effectively doubled. Using the same kickers and the same BPMs should also reduce the effects of BPM rotation on the extracted emittance, which give a spurious coupling term. This is partially cancelled when using information from both planes.

Analysis of the tolerances to different static effects, given in Table 2, shows that the effectiveness of the correction is generally reduced for most effects, but is markedly increased for the BPM rotation tolerance, as expected.

Table 2 Comparison of static tolerances between single-plane and dual-plane coupling correction.

Tolerance	**Single Plane Coupling Correction**	**Dual Plane Coupling Correction**
All Errors	2.02	1.89
Quadrupole Rotation	0.7mrad	0.74mrad
Sextupole Vertical	2788μm	2289μm
BPM Vertical	339μm	289μm
BPM Rotation	215mrad	315mrad

With almost twice as much information, the combined vertical dispersion and coupling matrix becomes very large. Optimising the matrix inversion in terms of the number of eigenvalues and the dispersion weighting becomes quite difficult. The decrease in tolerances seen in this case could be partly due to an imperfect matrix inversion. It is expected that with finer tuning of the matrix inversion parameters the correction can be improved so as to be at least as good as single-plane

coupling correction, and significantly better for specific tolerances such as the BPM and quadrupole rotations.

7.1 ATL Motion

Analysis of the ATL motion has also been performed with correction using the dual-plane coupling matrix. The results are shown in Figure 15. However, in this case correction is only performed every 3 days, rather than once per day. Comparison with Figure 9 shows that the extracted emittances are slightly higher, but this can obviously be compensated by correcting more often. Using dual-plane coupling matrices gives a roughly factor of 2 increase in the allowable time between correction, at the expense of a small increase in the tuning time.

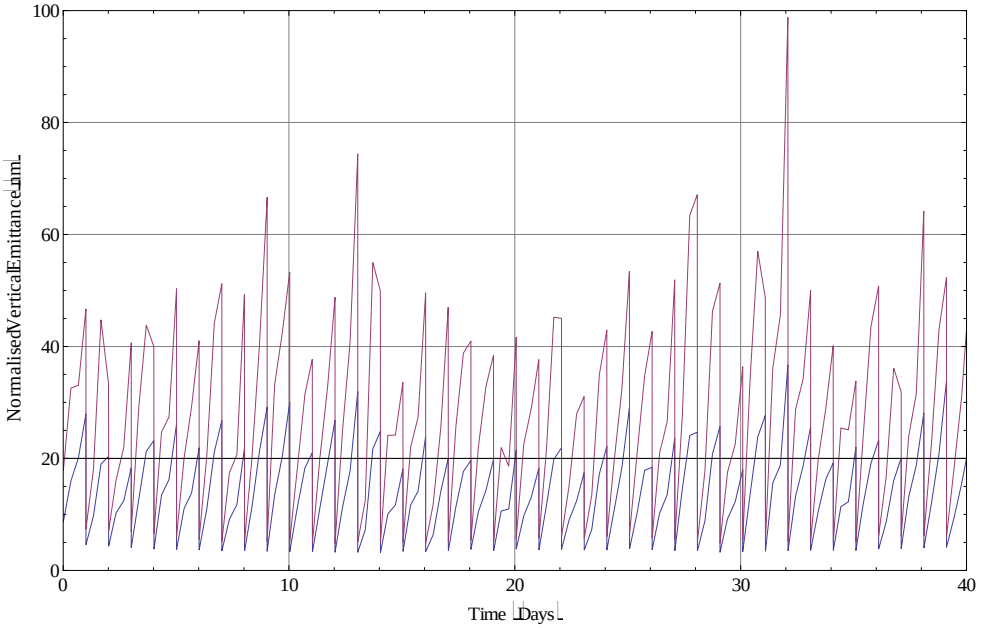

Figure 15 Plot of the normalised emittance from the damping ring over time under the influence of ATL ground motion. The r.m.s (blue) and the 95% confidence limit (magenta line) are shown, for 15 random seeds. Full closed-orbit and vertical dispersion and coupling correction is performed once every 3 days.

8 Conclusions

Analysis of the damping ring low emittance tuning has been performed with a candidate algorithm using response matrices for closed orbit correction, as well as vertical dispersion correction and coupling correction. The damping ring design has been analysed in terms of the tolerances to static errors, as well as dynamic errors arising from slow ground motion. The algorithm has been shown to produce extracted emittances significantly below the required value of 20nm, and with sufficient flexibility to relax the current tolerances.

The limits on the number of beam position monitors and skew quadrupole correctors have also been investigated, and in both cases, there is scope to reduce their number significantly and maintain the required vertical emittances.

Finally, an extension of the algorithm to provide more information for coupling correction has been shown to provide adequate emittance tuning in general, and to provide greater tolerance to spurious coupling measurements due to BPM rotations. The extended algorithm has also been shown to improve the long term dynamic tolerance of the damping ring, such that complicated and time-consuming correction can be performed less often.

9 Acknowledgement

This work is supported by the Commission of the European Communities under the 6th Framework Programme “Structuring the European Research Area", contract number RIDS-011899.

---

[i] https://wiki.lepp.cornell.edu/ilc/bin/view/Public/DampingRings/#Damping_Rings_Parameters_and_Lat

[ii] A. Wolski and N. Walker, “A MODEL OF ATL GROUND MOTION FOR STORAGE RINGS”, PAC 2003, Portland, Oregon.

[iii] J. Jones, “SLOW GROUND MOTION MODELLING OF DIAMOND”, PAC 2003, Portland, Oregon.

[iv] Y. Chung, G. Decker and K. Evans Jr., “Closed Orbit Correction Using Singular Value Decomposition of the Response Matrix”, PAC 1993, Washington, D.C.

[v] J. Jones, “TUNING ALGORITHMS FOR THE ILC DAMPING RINGS”, EPAC 2006, Edinburgh, Scotland.

[vi] See, for instance, proceeding of the “International Workshop on Beam Orbit Stabilisation” 2004, http://iwbs2004.web.psi.ch/